

NUCLEAR-ELECTRON COUPLING IN GAAS SPIN
STATES AND CONTROL OF THE EFFECTS

by

Benjamin M. Heaton

A senior thesis submitted to the faculty of

Brigham Young University

in partial fulfillment of the requirements for the degree of

Bachelor of Science

Department of Physics and Astronomy

Brigham Young University

August 2009

Copyright © 2009 Benjamin M. Heaton

All Rights Reserved

BRIGHAM YOUNG UNIVERSITY

DEPARTMENT APPROVAL

of a senior thesis submitted by

Benjamin M. Heaton

This thesis has been reviewed by the research advisor, research coordinator,
and department chair and has been found to be satisfactory.

Date

John S. Colton, Advisor

Date

Eric Hintz, Research Coordinator

Date

Ross L. Spencer, Chair

ABSTRACT

NUCLEAR-ELECTRON COUPLING IN GAAS SPIN STATES AND CONTROL OF THE EFFECTS

Benjamin M. Heaton

Department of Physics and Astronomy

Bachelor of Science

A brief introduction into quantum computing as well as the background for our experiments will be presented. The work discussed here will show dynamic nuclear polarization which affects the magnetic resonance properties of lightly doped n-GaAs spin states in both bulk and quantum well samples. The nuclear polarization affects spin lifetimes and the ability to use magnetic resonance as a spin manipulation technique. This nuclear polarization can be blocked through double resonance techniques.

ACKNOWLEDGMENTS

I'd like to thank John for his eternal patience with me and constant help with both the research and the writing of this paper.

Contents

Table of Contents	vi
1 History of Quantum Computing	1
2 How Quantum Computing Works	3
3 Where We Fit In	5
3.1 A qubit should have two states	5
3.2 We can perform qubit operations	6
3.3 Superposition	7
3.4 Preventing loss of information	7
4 Nuclear Effects Influence The Electron Spin Properties	9
5 A Forward to the following paper	10

Chapter 1

History of Quantum Computing

The setting and author of the first thoughts on quantum computing are hard to nail down exactly, but it is clear that interest was focused on the subject in 1981 when Richard Feynman spoke in a computing seminar at MIT. Here he articulated the sad fact that we will never be able to effectively model a quantum phenomenon with a classical computer. During the few years that followed some of the theoretical work was done by Deutsch and others showing how a quantum computer (QC) could be feasible. Still, there was little excitement on the subject until 1994 when Peter Shor showed the first really functional algorithm to be used by a quantum computer. Shor's algorithm could factor numbers. Although this may not sound exciting, his discovery led to the funding of research for much of the future work in this field. A computer that can efficiently factor very large numbers into primes will be able to easily crack the most commonly used encryption schemes.

This potential application has led many researchers towards developing ideas for hundreds of different "types" of quantum computers. In addition to the factoring algorithm, Grover developed a noteworthy algorithm for searching a database, and several other applications for possible future quantum computers have been dreamed

up. Still, for all of the effort put into the goal of making a working computer there are enough technical challenges to give job security for plenty of future physicists. For the past several years, quantum computing (and research motivated by it) held the attention of a significant percentage of the sessions at the APS conferences.

Chapter 2

How Quantum Computing Works

Classical computing uses charge and voltage to store and process information. In this case all data is represented as combinations of bits having either high or low voltage; we call these voltages 1's and 0's. Data is manipulated through operations which can change one bit by itself, or can have an output that is dependent on multiple inputs. Also we wouldn't want our data to change spontaneously on us. Similarly, quantum computing schemes must have the same three ingredients: 1) have at least two states, 2) be able to be acted on by both unary and binary operations, and 3) not lose information spontaneously. The computational advantages to quantum computing comes through the fourth ingredient: 4) the use of quantum superposition and entanglement.

Quantum bits (qubits, or qbits) are the quantum states that will be used as the bits in this computer. Really, any quantum mechanical property would work, but typically we would like our qubits to only have two possible states to make things easier (imagine a linear algebra space that is spanned by two basis vectors). In this case we will call the states $|0\rangle$ and $|1\rangle$, using the familiar Dirac notation.

Although entanglement is absolutely necessary for most proposed QCs, the topic

will not be discussed here (<http://www.ibm.com/developerworks/linux/library/l-quant.html> provides insightful examples and explanations for the advanced reader). I will give a very brief explanation of superposition and its power in quantum computing. In introductory courses in quantum mechanics as well as in linear algebra we learned about superpositions. Remember, because the x and y axis span a two dimensional space we can write any vector in 2-space as a superposition of \hat{x} and \hat{y} , $\alpha|\hat{x}\rangle + \beta|\hat{y}\rangle$. There is, however, nothing special about \hat{x} and \hat{y} . We could pick any two orthogonal vectors in the space and show that they span 2-space, like the cartesian vectors (1,1) called \vec{v} and (-1,1) called \vec{w} . $|\vec{v}\rangle$ and $|\vec{w}\rangle$ work as basis vectors where any other vector in the space can be written as $\alpha|\vec{w}\rangle + \beta|\vec{v}\rangle$. Even $2|\hat{y}\rangle = |\vec{w}\rangle + |\vec{v}\rangle$.

In QC this becomes very powerful because one state can be an equal superposition of every possible state in the orthogonal basis. Here is a simple illustration. Imagine you had a time-consuming guess and check algorithm with many possible inputs. Instead of running the algorithm on each possible solution separately, you could just represent your input in an orthogonal basis (a superposition of every possible input), run your algorithm once, transform back into the original basis, and then measure the outcome. Although that sounds convoluted, a quantum computer makes it possible to check every possible guess at the same time. Obviously this example isn't 100 percent correct, but it illustrates the basic idea.

One of the major challenges in QC has been the random loss of information from qubits. This happens in classical computers too, but at rates slow enough to allow for error correcting codes to fix the problem. If QCs are to become a reality then qubits must be able to retain their information for relatively long periods of time.

Chapter 3

Where We Fit In

One of the proposed candidates for qubits in the future's QCs is the electron spin properties in certain semiconductors. We have been studying the spin states in GaAs samples. These quantum mechanical spin states fit all four of the ingredients listed in "How Quantum Computing Works": they have two states, they can be manipulated, they don't lose their information, and they can take advantage of superposition and entanglement.

3.1 A qubit should have two states

Our research has touched on aspects of each of the four main ingredients required for a good qubit. In a strong magnetic field the electron spin is split into two distinct energy states. This is familiar to us as Zeeman splitting, and these lower and higher energy states can be our $|0\rangle$ and $|1\rangle$. A large portion of our work has been in doing experiments that cause our electron spins to transition from $|0\rangle$ to $|1\rangle$ and back.

Figure 1 (in the paper towards the end of this document) shows the two spin states during an optically detected magnetic resonance (ODMR) scan. The two different

curves in this graph show two separate experiments plotted together for comparison. The signal being plotted on the y-axis is a measure of the spin polarization of the electrons in our GaAs sample, and the x-axis shows the external magnetic field that was our variable. The spin state in these experiments is measured through use of a probe laser beam, which reflects off of the sample. As the beam is reflected, the axis of polarization of the linearly polarized light is rotated proportional to the electron spin polarization in the sample; this effect is called Kerr rotation. The resonance curve seen in the figure clearly shows that the magnetic field induced a transition to a higher energy spin state at one specific field strength. This magnetic resonance occurs because the sample is being pumped with energy from a microwave source, and when the external B-field causes Zeeman splitting between the two energy states to exactly match the supplied microwave energy, then the electron can jump to the higher energy state. In our experiments, the electrons are initialized to the lower energy state prior to the resonant conditions, because the temperature of the sample is typically kept at 1.5 K (kBT is on the order of the Zeeman energy splitting)

3.2 We can perform qubit operations

The ODMR experiments are unary QC operations which we can successfully control (under certain conditions). We have also been working on spin-echo and Rabi flopping experiments which also demonstrate control of the spin states. Rabi flopping is little more than a manifestation of absorption and stimulated emission. Einstein discovered, in 1917, that if a photon of the right energy hits a two level system it will cause a transition, even if the system was already in the higher energy state. So the first photon to hit a system will cause a transition $|0\rangle \rightarrow |1\rangle$ (absorption), the second photon will cause the transition $|1\rangle \rightarrow |0\rangle$ (emission), the third back to

$|1\rangle$, and so on as the state flops back and forth. Actually observing Rabi flopping in our samples has proved to be very difficult, and so far we have not seen conclusive evidence of this effect.

3.3 Superposition

So far we have touched on two of the four ingredients. Again, I will not discuss entanglement in our experiments, but we have been touching on the idea of superposition in our spin-echo experiments. In the last section we talked about Rabi flopping as a very discreet process, but in real life each photon absorbed gives a probability of transition and we have many electrons and photons in our system. This probabilistic absorption leads to a very continuous oscillation of the percentage of total spins in the $|1\rangle$ state. This oscillation also occurs at a characteristic rate called the Rabi frequency. A spin-echo experiment uses the knowledge of the Rabi frequency to manipulate the spin states. A pulse of transition causing photons that is exactly as long as the Rabi frequency will cause a 2π rotation back to the original state. A π pulse will cause one flop ($|0\rangle \rightarrow |1\rangle$) and a $\pi/2$ pulse will rotate the spin state halfway between the two states. In our physical experiment where $|0\rangle$ could be spin down and $|1\rangle$ could be spin up, halfway would put the spin in an orthogonal plane where it would be measured to be $|0\rangle$ 50% of the time and $|1\rangle$ 50% of the time. Now our qubit is in a superposition of the two states.

3.4 Preventing loss of information

All of the experiments previously described have been done as stepping stones towards the goal of measuring the lifetime of the spin states in GaAs. The samples that we

have been studying are only possible candidates to become qubits if they can exist for relatively long periods of time (microseconds in our case) without losing information. This is called the spin lifetime. The information is “lost” when a qubit interacts with its environment in some way causing it to change its spin state. This lifetime of an electron spin state can be classified into three separate lifetimes. The spin flip time, called T_1 , is the time it takes for the spin state to randomly switch from $|1\rangle$ to $|0\rangle$. The T_2 lifetime is the time before there is loss of spin phase information and is relevant to QC, and this time is what we would like to be able to measure for this sample. There is also a time T_2^* which is similar to T_2 , but has been shortened by inhomogeneous effects that can be overcome. All of the ODMR, Rabi, spin-echo, and other experiments that have or will be discussed in this paper are part of the process towards being able to measure the T_2 lifetime for our GaAs sample.

Chapter 4

Nuclear Effects Influence The Electron Spin Properties

There has been one problem which we have spent much of our recent efforts trying to overcome. The GaAs electron spin states are influenced by their environment. Particularly, they get feedback from the spin states of the Ga and As nuclei in the sample. This electron-nuclear spin state coupling is called the Overhauser effect. It happens as the electron spins align and create a net field along their dipole moment. This net field tends to align the nuclear spins, which changes the local environment for the electron spins. This feedback through Overhauser coupling leads to dynamic nuclear polarization (DNP) which has made the T_2 measurements more difficult.

We have achieved partial control over the effects of DNP, but there is still much work to be done in this area.

Chapter 5

A Forward to the following paper

This document so far has been intended to be an introduction providing some brief background information on my research topic. The next few pages are a paper that I have written on the work done as my senior thesis project. This paper will serve as the culmination of my work at BYU on this project. This paper will be submitted to the Applied Physics Letters journal in September 2009.

Nuclear-Electron coupling in GaAs spin states and control of the effects

Benjamin Heaton and John S. Colton

(Dated: August 7, 2009)

We have observed dynamic nuclear polarization which affects the magnetic resonance properties of lightly doped n-GaAs spin states in both bulk and quantum well samples. The nuclear polarization affects spin lifetimes and the ability to use magnetic resonance as a spin manipulation technique. This nuclear polarization can be blocked through double resonance techniques.

PACS numbers:

Applications in spintronics and quantum information can further develop if electron spin states can be manipulated and have good spin properties. A long spin decoherence lifetime is essential to prevent loss of information during the application or manipulation of the information[1].

n-type GaAs is a good candidate for long lifetime spin states as has been shown by the long T_1 and T_2^* lifetime previously reported[2]. Long T_1 lifetimes have been obtained using lightly doped n-type samples where the electron densities are low enough to mimic the quantum dot case.

The samples described in this letter are a 1 micron thick $3 \times 10^{14} \text{ cm}^{-3}$ silicon-doped bulk GaAs layer as well as a $3 \times 10^{10} \text{ cm}^{-2}$ modulation-doped quantum-well (QW) sample. These two samples have been studied by several groups which have shown some of the spin and physical properties of samples [3][4][5][6]. Both samples were grown by molecular beam epitaxy at the Naval Research Lab. The active regions are surrounded by AlGaAs layers. The quantum-well sample has wells of 2.8, 4.2, 6.2, 8.4, and 14 nm[7]. All of our results on the quantum-well sample were done on the 14 nm well, which was selected by tuning the probe laser to match the exciton wavelength of that well.

Electron spin resonance techniques (ESR), including optically detected magnetic resonance (ODMR), provide a well-established tool for manipulating spins. This can be employed for measuring lifetimes and performing operations on the quantum state. The magnetic resonance experiments described in this letter were detected through Kerr rotation, the rotation of the angle of polarization of a linearly polarized probe beam in response to the magnetization or spin polarization of a sample. Kerr rotation is measured in reflection but is otherwise similar to Faraday rotation in transmission. Our Kerr rotation technique measured by cw laser is otherwise similar to the pulsed laser Kerr rotation measurements made by Kennedy et al.[3]

To detect magnetic resonance by Kerr rotation we first create initial spin polarization of the sample by placing it in a 1.4–1.9 Tesla magnetic field generated by an Oxford Instruments Spectromag. When cooled to 1.5 K, Boltzmann statistics predict the polarization of electron spins to be $\frac{n_{\uparrow} - n_{\downarrow}}{n_{\uparrow} + n_{\downarrow}} = \tanh \frac{g\mu_B B_{\text{ext}}}{2k_B T} = 0.18$ at 1.76 T, the magnetic resonance field of the QW sample when resonated at 11 GHz [Fig. 1]. A Spectra Physics tunable cw Ti-

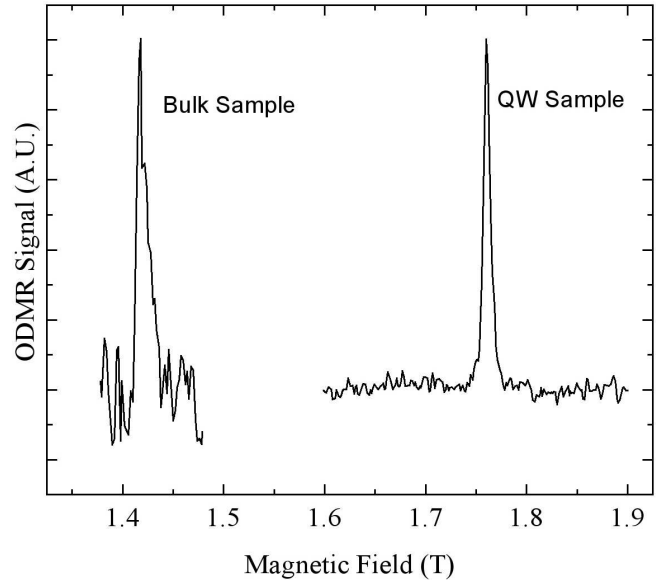


FIG. 1: Typical ODMR scans for each type of sample done at 1.4 K. Each sample is resonated at 11 GHz, so two samples with the same g-factor would have the same magnetic resonance field; this highlights the different g factors.

sapphire laser is tuned to 821 nm for bulk sample or 807 nm for the QW sample. These wavelengths were chosen to optimise the Kerr rotation signal; the 821 nm is a few nm below the exciton wavelength of the bulk sample while the 807 nm is on the exciton wavelength for the QW. The beam is directed parallel to the axis of the external magnetic field, and the external magnetic field causes the spin states to split by $\Delta E = g\mu_B B$. Resonance occurs when microwaves at about 10 GHz cause spin flip transitions between the two energy states, changing the overall polarization. A custom made microwave cavity is used to enhance the microwave field at the sample (for details on the resonator construction see [8]). The spin polarization change is measured in the Kerr rotated probe beam by a polarization beam splitter and a balanced detector.

A spin resonance experiment shows the g-factor from the peak position and T_2^* from the peak width and position. $T_2^* = \frac{\hbar}{(g\mu_B B_{1/2})}$ [9] [Fig. 1]. The g factor for the bulk and QW sample was $|g| = 0.42$ and 0.35 respectively. The T_2^* for the bulk and QW sample was 22 ns and 23 ns respectively. These results for the QW sample,

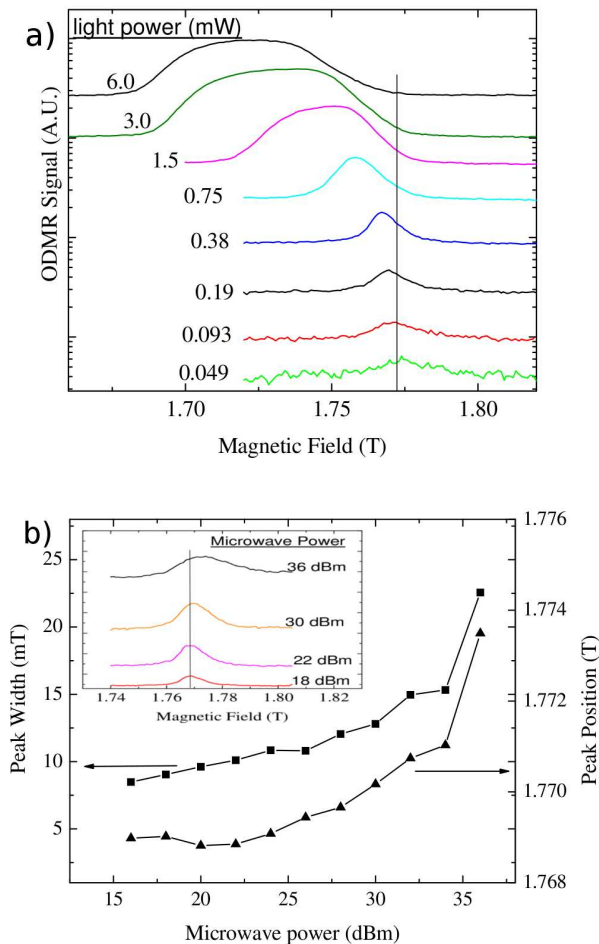


FIG. 2: Overhauser coupling causes DNP related broadening and shifting of the ODMR peak. (a) As the probe laser power increases, the DNP increases. (inset to b) As the resonating microwave power increases the change in electron polarization percentage causes DNP, which causes the shifting and broadening. The analysis of ODMR peak width and position as a function of resonating microwave power show the limits of no DNP to give a minimum peak width of near 7 mT and peak position of 1.769. This corresponds to $|g| = 0.347$ and $T_2^* = 9\text{ns}$ for the QW sample.

although different from the bulk sample properties[3] are in line with what was expected. The difference in the g factor is from the exciton's interaction with the surrounding AlGaAs layers which have a g factor of the opposite sign from GaAs, so the QW g factor is closer to zero than the bulk g factor.

Both the quantum well and the bulk sample showed dynamic nuclear polarization (DNP) from Overhauser coupling which occurs when the electron spin polarization is taken out of equilibrium [10]. This hyperfine coupling between a the spin of a localized electron and the nuclear spins within its interaction radius creates a shift in the external field needed to fulfill the resonance condition $hf = g\mu_B B_{net}$ where B_{net} is the sum of both the

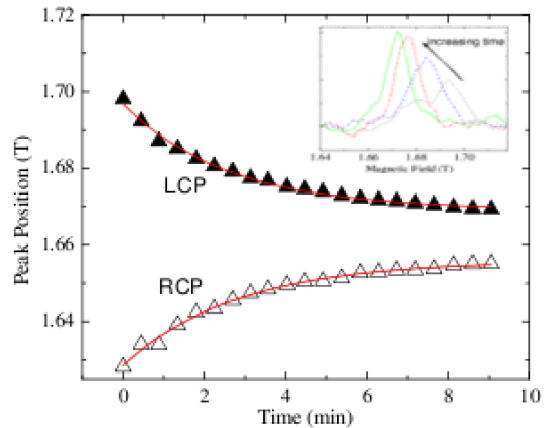


FIG. 3: Under conditions of strong DNP the ODMR peak has shifted away from the equilibrium resonant field (to the right, in the inset). Over time the nuclear polarization relaxes and the ODMR peak shifts back towards the equilibrium position at a characteristic nuclear relaxation rate of 2.7 minutes. This technique used both right and left circularly polarized light to cause DNP shifting to lower and higher (respectively) resonant magnetic fields. The apparent difference between the two equilibrium magnetic fields is an artifact of the data collection rate; the true ODMR field with no DNP is near 1.66 T, the average of the two equilibrium points shown.

applied magnetic field and the local field which is directly proportional to the nuclear spin polarization. As seen in Figure 4 a higher laser powers lead to a shift in the measured ODMR field position. The DNP increases with increasing laser power as the fraction of resonated electrons increases showing a larger shift in the effective resonant field. Local inhomogeneity in the nuclear polarization, caused in part by the gaussian profile of the probe laser beam, is manifested as broadening of the ODMR peak. The flattening of the peaks at higher laser powers in Figure 4 is a result of the DNP happening in real time as the scan over magnetic field values follows the effective resonant field. The DNP related shift and broadening occurs with increasing probe laser power and with increasing microwave resonating power.[Fig. b.]

Since the shift in the ODMR peak position is directly proportional to the nuclear spin polarization, fast low-power ODMR scans can be used to measure the nuclear spin relaxation time. To do this we first polarized the nuclei by pumping with a circularly polarized laser. Figure 3 shows this can shift the ODMR peak to higher or lower magnetic fields depending on the polarization orientation of the pump beam. The ODMR peak position was monitored in time as it shifted back to the equilibrium resonant magnetic field. It did so with a characteristic time of 2.7 minutes. [Fig 3].

We observed less shifting and broadening of the ODMR peak in the QW sample than in the bulk sample under similar conditions. This indicates less DNP, which is

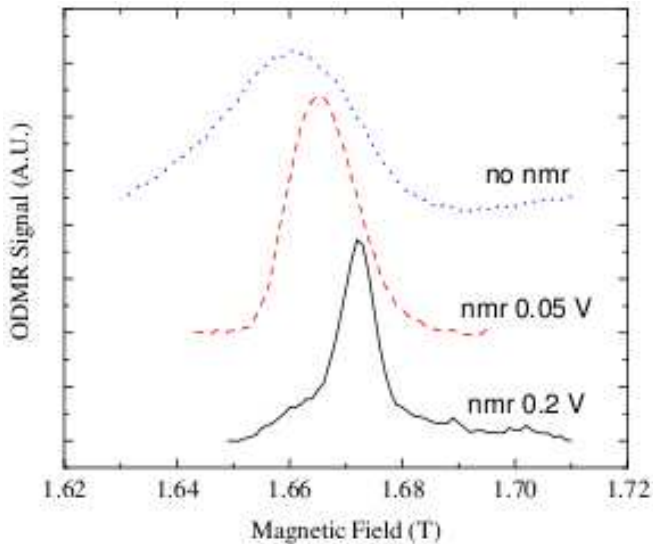


FIG. 4: Demonstration of the NMR reducing DNP. Under conditions of strong DNP the ODMR peak is broadened and shifted. As the NMR frequencies are resonated the nuclei are randomized, reducing the DNP. This nuclear randomization is directly proportional to the radio frequency voltage applied.

consistent with the reduced hyperfine effects one expects in samples where the electron wavefunctions are closer together. Still, the dramatic effects of this Overhauser coupling [Fig.] place serious limits on the spin manipulation of both samples and on the practical use of these materials in future applications. This can be reduced by simultaneously resonating the nuclei with the electrons to reduce the DNP. Resonating the nuclei randomizes the nuclear spin polarization and blocks the DNP. Nuclear magnetic resonance (NMR) was performed by placing the sample in a split Helmholtz coil (seven turns on each side) that was electrically driven to create oscillating magnetic fields at 14, 19, and 25 MHz, the NMR frequencies for the three nuclear isotopes in our sample, ^{75}As , ^{69}Ga , and ^{71}Ga . Simultaneously sweeping through the NMR frequencies while doing an ESR scan was able to eliminate the peak shifting and broadening caused by the Overhauser coupling in many cases, although conditions of strong DNP due to high probe beam powers or microwave resonating powers make this more difficult. Figure 4 shows that stronger NMR fields were able to resonate a higher percentage of the nuclei and therefore eliminate more of the effects of the DNP.

The electron-nuclear interaction can also be observed through the nuclear resonance. To show this we set the magnetic field to the ODMR peak. While the RF signal was scanned through the three nuclear resonant frequencies, the electron ODMR signal was monitored. (This is similar to a typical Optically-detected electron-nuclear double resonance, ODENDOR, experiment.) The chang-

ing nuclear polarization as each nuclear resonance condition was met affected the electron spin polarization and was seen in the ODMR signal. Fig. 5 illustrates a varia-

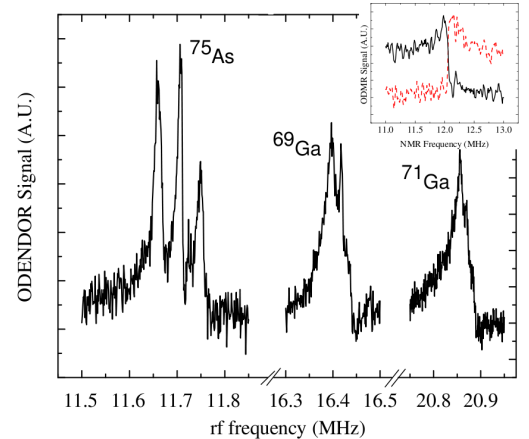


FIG. 5: The ODMR signal shows the NMR frequencies, during double resonance experiments. The inset shows only the nuclear magnetic resonance for the ^{75}As isotope. In the main figure the first peak shows splitting into three sub-peaks; this is predicted by theory but the splitting shown is too large and is likely an artifact of the data collection methods.

tion of this experiment. In this case we first polarized the nuclei shifting the ODMR peak away from equilibrium. Then we monitored the ODMR signal while resonating the NMR frequencies for two of the three nuclei continuously and slowing sweeping through the third NMR frequency. While keeping the magnetic field at the equilibrium ESR value and stepping through the third NMR frequency, the ODMR signal increased dramatically when the third nuclei was resonated and the DNP was eliminated. This is the sharp increase in signal in Fig. 5. The two curves in this figure show the NMR frequency for As as found by sweeping both up and down through the NMR frequency.

In summary, we have used Kerr rotation to measure magnetic resonances in both bulk GaAs and 14 nm quantum-well GaAs. We have measured the g-factor and T_2^* to be 0.42 and 22 ns in the bulk sample and 0.35 and 23 ns in the QW sample. The DNP is a significant effect which cannot be ignored in spin studies as it leads to changing the electron magnetic resonance and inhomogeneous shortening of T_2^* . The nuclear polarization relaxation time is 2.7 minutes. Double resonance of the electrons and nuclear isotopes can block DNP and can be used to study nuclear spin properties. The control of the nuclear spin states is required for future study of electronic spin properties since these two systems are directly coupled.

-
- [1] a. D. D. D. Loss, Phys. Rev. A **57** (1998).
[2] J. Kikkawa, Phys. Rev. Lett. **80** (1998).
[3] Kennedy, Phys. Rev. B. **74** (2006).
[4] J. G. Tischler, A. S. Bracker, D. Gammon, and D. Park, Phys. Rev. B **66**, 081310 (2002).
[5] R. I. Dzhioev, K. V. Kavokin, and e. a. Korenev, Phys. Rev. B **66**, 245204 (2002).
[6] T. A. Kennedy, A. Shabaev, M. Scheibner, A. L. Efros, A. S. Bracker, and D. Gammon, Physical Review B (Condensed Matter and Materials Physics) **73**, 045307 (pages 6) (2006), URL <http://link.aps.org/abstract/PRB/v73/e045307>.
[7] J. Tischler, Phys. Rev. Lett. **66** (2002).
[8] J. Colton, Rev. Sci. Instrum **80**, 035106 (2009).
[9] J. C. et al, Solid State Communications **132**, 613 (2004).
[10] B. Clerjoud, Phys. Rev. B. **40** (1989).